UNCLASSIFIED

AD **404 917**

DEFENSE DOCUMENTATION CENTER

FOR

SCIENTIFIC AND TECHNICAL INFORMATION

CAMERON STATION, ALEXANDRIA, VIRGINIA

UNCLASSIFIED

MEMORANDUM
RM-3525-PR
APRIL 1963

CLOSE-IN ELECTROMAGNETIC FIELDS
PRODUCED BY NUCLEAR EXPLOSIONS

W. Sollfrey

PREPARED FOR:

UNITED STATES AIR FORCE PROJECT RAND

The RAND *Corporation*

SANTA MONICA • CALIFORNIA

MEMORANDUM
RM-3525-PR
APRIL 1963

CLOSE-IN ELECTROMAGNETIC FIELDS
PRODUCED BY NUCLEAR EXPLOSIONS

W. Sollfrey

The RAND *Corporation*

1700 MAIN ST · SANTA MONICA · CALIFORNIA

PREFACE

The study reported in this Memorandum is an outgrowth of RAND's continuing interest in the electromagnetic effects of nuclear explosions. It should be useful to students of the theoretical aspects of systems designed to function in the environment of such explosions.

SUMMARY

The close-in electromagnetic fields produced by deflection in the earth's field of Compton electrons from a nuclear explosion are analyzed. Maxwell's equations in spherical coordinates are solved by an expansion in the perturbation fields, taking into account the space and time dependence of the conductivity and Compton current. The field structure is determined, and it is shown that the peak change in field is only 10 per cent.

ACKNOWLEDGMENTS

It is a pleasure to acknowledge many helpful discussions with
R. Bjorklund, C. Crain and W. Karzas, all of the RAND Corporation.

ix

CONTENTS

LIST OF FIGURES

LIST OF SYMBOLS

a	half the ratio of the gamma-ray mean free path and the characteristic length associated with the conductivity
$\vec{B}$	vector magnetic induction (webers/meter^2)
B	earth's magnetic induction
B_r	radial component of magnetic induction
ΔB_r	perturbation in radial component of magnetic induction
B_θ	latitudinal component of magnetic induction
ΔB_θ	perturbation in latitudinal component of magnetic induction
c	velocity of light (meters/second)
$\vec{E}$	vector electric field (volts/meter)
E	magnitude of vector electric field
E_ϕ	azimuthal component of electric field
e	charge on electron (coulombs)
F	function related to the vector potential function
F_o	lowest order term in expansion of F
F_1	next lowest order term in expansion of F
f	gamma-ray production rate
G	e^{-x}/x^2, function characterizing space dependence of conductivity and current
g	function characterizing retarded time dependence of conductivity
g_o	constant related to the peak value of g
h	function characterizing retarded time dependence of current
I	integral of G
$\vec{i}_r$	unit vector in the radial direction
$\vec{i}_\phi$	unit vector in the azimuthal direction

$\vec{J}$ current density vector (amperes/meter^2)

J_o constant related to peak value of current

m   mass of electron (kilograms)

n   electron number density (meter^{-3})

p   pressure

q   secondary electron multiplicity factor

R   range of Compton electrons (meters)

r   radial distance coordinate (meters)

r_e value of r at which a field line cuts the equatorial plane

T   characteristic attachment time (seconds)

t   time (seconds)

$\vec{v}$ electron velocity vector (meters/second)

v_o radial electron velocity

W   function characterizing field space and time dependence

x   normalized radial distance

x_1 normalized radius of ionization sphere

y   normalized time

β attachment rate constant (seconds^{-1})

γ relativistic parameter of Compton electrons

θ latitudinal coordinate

λ mean free path of gamma-rays (meters)

μ permeability of free space (henry/meter)

ρ relabeled radial coordinate

σ conductivity (mho/meter)

τ retarded time (seconds)

ϕ azimuthal coordinate

ψ function which determines ionization radius

ω_e electron mobility [(meters/second)/(volt/meter)]

I. INTRODUCTION

It is well known that nuclear explosions may produce appreciable electromagnetic signals.[1,2] The theory has been developed for the electromagnetic radiation from nuclear explosions at high altitudes or in space,[3-5] and also for Compton electron interactions with the earth's field.[6] However, most of the theory deals with electric fields or dipole radiation fields. This Memorandum considers the near magnetic fields. The principal mechanism treated is Compton electron interaction.

The approximations used in the analysis restrict the solution to early times. However, the fields may be expected to be strongest shortly after the arrival of the gamma rays, so these results represent the most significant portions of the field. The nature of the analysis is such that the results should be upper bounds on the actual fields.

II. CLOSE-IN ELECTROMAGNETIC FIELDS PRODUCED BY COMPTON ELECTRONS

The analysis will be devoted primarily to the possible exclusion of the earth's magnetic field by the electrons produced by the nuclear blast. To avoid great complications, the effect of the proximity of the conducting earth will be neglected. If the earth is highly conducting, the image charges induced in it will tend to cancel the horizontal electric and vertical magnetic fields near the surface, and to augment the vertical electric and horizontal magnetic fields by a factor near 2. These effects may be considered in a future Memorandum.

If the proximity of the earth is neglected, the gamma rays produced by the blast will be emitted primarily in the radial direction. These gamma rays will be scattered and absorbed in the atmosphere, producing Compton electrons. We shall only consider low-altitude blasts, for which the variation of atmospheric density with altitude will be neglected. Since the scale height is about 8.4 km, and we are interested in heights below 3 km, this is a reasonable assumption. Under these circumstances, the atmospheric conductivity will only be a function of time and distance from the blast. In MKS units, the conductivity is given by:

$$\sigma(t,r) = e \; \omega_e \; n(t,r) \tag{1}$$

where e is the electron charge in coulombs, ω_e the electron mobility in (meters/sec)/(volts/meter), and n(t,r) is the number of electrons per cubic meter at the distance r from the burst point at the time t.

The proper value of mobility to employ is somewhat uncertain. The electrons are rapidly slowed down by collisions, and then they become attached to oxygen via a three-body reaction. The duration of this process is about 1 shake (10^{-8} sec). Measurements of the electron mobility in air[7-10] indicate that the mobility and also the electron attachment rate are energy-dependent.

The data are given as functions of the ratio of electric field strength, E, to pressure, p. At atmospheric pressure, and the field strengths estimated to be produced by a 1-MT blast, E/p is so low that there simply are no published measurements in this region, and it is necessary to extrapolate the curve. There is appreciable curvature in the mobility curve at the lowest values of E/p for which there are data, so the extrapolation may be subject to error. There is also some evidence of a cutoff in the collision process, which causes the mean energy of the electrons to be higher and changes the effective mobility. In all, estimates of the mobility may be in error by a factor of 2 or 3. After discussions with R. Bjorklund and W. Karzas on the data extrapolation process an average value of .20 meters^2/volt-sec has been selected for the calculations. The electron density produced by a 1-MT burst has been calculated from Eq. (4) of Ref. 6; and the conductivity at selected values of distance and time is listed in Table 1. The time is in shakes, measured from the initiation time r/c, and the distance is in kilometers.

These data have been deduced from the expression

$$\sigma = G(r) \; g(t - \frac{r}{c}) \qquad\qquad (2)$$

Table 1

ATMOSPHERIC CONDUCTIVITY (MHO/METER) PRODUCED BY A 1-MT EXPLOSION

Time, t, Shakes	Distance, r, from burst point, km								
	0.5	0.75	1.0	1.25	1.5	1.75	2.0	2.5	3.0
1	1.6(-1)	2.9(-2)	6.3(-3)	1.6(-3)	4.0(-4)	1.1(-4)	3.7(-5)	6.0(-6)	9.3(-7)
2	1.7	3.3	7.0	1.9	5.0	1.4	4.0	6.7	1.2(-6)
5	1.6	2.9	6.3	1.7	5.0	1.5	4.3	6.0	1.3
10	1.3	2.4	5.3	1.4	4.3	1.4	4.3	5.0	1.1
20	9.0(-2)	1.7	3.8	1.1	3.3	1.1	3.8	4.5	8.3(-7)
50	3.8	7.7(-3)	2.2	6.7(-4)	2.2	8.0(-5)	3.0	4.0	6.3
100(1 μ sec)	2.3	5.0	1.4	4.8	1.7	6.3	2.5	3.8	5.7
200	1.6	3.7	1.1	3.7	1.3	5.0	2.1	3.6	5.0
500	6.7(-3)	2.1	4.7(-4)	1.6	5.8(-5)	2.4	1.1	2.2	3.7
1.0(3)	1.6	4.0(-4)	1.2	4.0(-5)	1.7	7.8(-6)	4.1(-6)	1.3	2.8
2.0(3)	9.7(-5)	2.7(-5)	9.3(-6)	4.7(-6)	2.7(-6)	1.9	1.4	7.3(-7)	2.3
5.0(3)	5.2(-6)	1.9(-6)	1.0(-6)	7.3(-7)	5.7(-7)	5.0(-7)	4.3(-7)	3.7	1.7
1.0(4)	5.2	1.9	6.7(-7)	4.3	3.1	2.5	2.2	1.8	1.2

Numbers in parentheses denote powers of 10

$$G(r) = e^{-(r/\lambda)}/(r/\lambda)^2 \tag{3}$$

$$g(t - \frac{r}{c}) = g_0 \int_0^{t-\frac{r}{c}} d\,t'\, f(t - \frac{r}{c} - t')\, e^{-\beta\,t'} \tag{4}$$

where λ is the mean path for removal of the gamma rays (300 meters), β is the attachment rate of the electrons (10^8 sec^{-1}), g_0 is a constant which is related to the peak value of the conductivity, and $f(t)$ is the normalized production rate of the gamma rays. For the listed data, a good value for g_0 is 130, while the time dependence of g is rather complicated. A characteristic time to represent the rise of g is 2 shakes, while the decay time is on the order of 20 shakes.

In these units, the Maxwell equations are:

$$\nabla \times \vec{B} = \frac{1}{c^2} \frac{\partial \vec{E}}{\partial t} + \mu(\sigma \vec{E} + \vec{J}) \tag{5}$$

$$\nabla \times \vec{E} = -\frac{\partial \vec{B}}{\partial t} \tag{6}$$

where μ is the permeability ($4\pi \times 10^{-7}$), c the velocity of light, $\vec{J}$ is the Compton current density (amps/meter^2), $\vec{E}$ the electric field (volts/meter) and $\vec{B}$ the magnetic induction (webers/meter^2).

The Compton electrons will be deflected by the local magnetic field. Practically all of the effect is due to the primaries, since the secondaries undergo very little deflection, and the deflection contributions in the two directions perpendicular to the magnetic field roughly balance. Following Karzas and Latter[6] the Compton current is given by:

$$\vec{J}(t,r) \sim J_o \, G(r) \, f(t - \frac{r}{c}) \int_o^{\max \, (t - \frac{r}{c}, \, \frac{R}{c})} d \, t' \, \vec{v}(t') \qquad (7)$$

where the velocity of the Comptons has been set equal to c in the production function. J_o is a constant, G and f are as in Eq. (2). The upper limit of the integral is equal to the larger of $t - \frac{r}{c}$ and $\frac{R}{c}$, where R is the range of the Comptons. Since $R \sim 1$ meter at sea level, the approximation $R/\lambda \ll 1$ has been made (actually, $R/\lambda \sim .01$). For the listed data, the constant J_o is 6×10^{-4}.

The Comptons are scattered radially from their point of origin. Take a system of spherical coordinates, with the origin at the burst point, and the polar axis along the earth's magnetic field; then the velocity of the deflected electrons is approximately:

$$\vec{v} \sim v_o \, \vec{i}_r + \frac{e \, B \, \gamma \, v_o \, t'}{m} \sin \theta \, \vec{i}_\phi \qquad (8)$$

Thus the deflection is in the azimuthal direction, has a latitude dependence sin θ, and the entire system is azimuthally symmetric.

Under these conditions, the Maxwell equations split into two groups, one involving the radial electric, latitudinal electric, and azimuthal magnetic fields; the second involving the azimuthal electric, latitudinal magnetic and radial magnetic fields. The first is driven by the radial current, the second by the azimuthal current. If the radial current is only a function of distance and time, as it is to this approximation, the first group of equations reduces to Poisson's equation, involves no magnetic fields, and will not be considered further.

In the spherical coordinates, the second group of equations may be written as:

$$\frac{1}{r \sin \theta} \frac{\partial}{\partial \theta} \sin \theta \, E_{\emptyset} = -\frac{\partial B_r}{\partial t} \tag{9}$$

$$\frac{1}{r} \frac{\partial}{\partial r} r \, E_{\emptyset} = \frac{\partial B_{\theta}}{\partial t} \tag{10}$$

$$\frac{1}{r} \frac{\partial}{\partial r} r \, B_{\theta} - \frac{1}{r} \frac{\partial B_r}{\partial \theta} = \frac{1}{c^2} \frac{\partial E_{\emptyset}}{\partial t} + \mu \, G(r) \left[g(t - \frac{r}{c}) \, E_{\emptyset} \right.$$

$$\left. + h(t - \frac{r}{c}) \sin \theta \right] \tag{11}$$

$$h(t - \frac{r}{c}) = J_0 f(t - \frac{r}{c}) \frac{e \, B \, \gamma \, v_0}{2 \, m} \cdot \max \left[(t - \frac{r}{c})^2, (\frac{R}{c})^2 \right] \tag{12}$$

Our task is now to solve these equations with the appropriate initial conditions. For $t < \frac{r}{c}$, the electric field, conductivity, and current vanish, while the magnetic field is uniform. The angular dependence is established by the factor $\sin \theta$ in the current. A representation which integrates the first two equations is:

$$E_{\emptyset} = \frac{\sin \theta}{r} \frac{\partial}{\partial t} F(t, r) \tag{13}$$

$$B_{\theta} = -B \sin \theta + \frac{\sin \theta}{r} \frac{\partial}{\partial r} F(t, r) \tag{14}$$

$$B_r = B \cos \theta - \frac{2 \cos \theta}{r^2} F(t, r) \tag{15}$$

where F satisfies the wave equation

$$\frac{\partial^2 F}{\partial r^2} - \frac{2F}{r^2} = \frac{1}{c^2} \frac{\partial^2 F}{\partial t^2} + \mu \, G(r) \left[g(t - \frac{r}{c}) \frac{\partial F}{\partial t} + r h(t - \frac{r}{c}) \right] \tag{16}$$

with the initial conditions

$$F = \frac{\partial F}{\partial t} = 0 \qquad t = \frac{r}{c} \qquad (17)$$

F is related to the vector potential function.

Introduce as new variables the distance r, which will be re-labeled ρ, and the delayed time $\tau = t - \frac{r}{c}$. The wave equation expressed in these variables is

$$\frac{\partial^2 F}{\partial \rho^2} - \frac{2F}{\rho^2} - \frac{2}{c} \frac{\partial^2 F}{\partial \rho \partial \tau} = \mu\, G(\rho) \left[g(\tau) \frac{\partial F}{\partial \tau} + \rho\, h(\tau) \right] \qquad (18)$$

with the initial conditions:

$$F = \frac{\partial F}{\partial \tau} = 0 \qquad \tau = 0 \qquad (19)$$

The solution obtained by Karzas and Latter[6] is equivalent to neglecting the left side of this equation. We wish to determine the effect of this neglect.

For this purpose, consider characteristic lengths and times. The ρ dependence is characterized by the mean free path λ(300 meters). The current and conductivity are characterized by times between 2 and 20 shakes, or equivalent lengths 6 and 60 meters. Therefore, the τ variation is fast compared to the ρ variation. Let us introduce dimensionless variables by:

$$\rho = \lambda\, x \qquad \lambda = 300 \text{ meters,} \qquad 1 \leq x \leq 10 \qquad (20)$$

$$\tau = T\, y \qquad T = 10^{-8} \text{ sec} \qquad 0 < y \leq 2000 \qquad (21)$$

where the inequalities indicate the expected range of values of significance of the variables. The wave equation becomes:

$$\frac{cT}{\lambda} \left(\frac{\partial^2 F}{\partial x^2} - \frac{2F}{x^2} \right) - 2 \frac{\partial^2 F}{\partial x \, \partial y} = \mu \, c \, \lambda \, G(x) \left[g(y) \frac{\partial F}{\partial y} \right.$$

$$\left. + \lambda \, T \, x \, h(y) \right] \qquad (22)$$

The essential point of the transformation is that $c \, T/\lambda = .01$. It may be expected that derivatives with respect to x and y are of the same order of magnitude. If we are not too close to the origin, say $x > 1$, the term involving x^{-2} is on the same order of magnitude as the x-derivative term. It is therefore plausible to expand the solution in powers of $c \, T/\lambda$, and keep only the first two terms. The equation splits as follows:

$$F = F_0(x,y) + \frac{cT}{\lambda} F_1(x,y) \qquad (23)$$

$$\frac{\partial^2 F_0}{\partial x \, \partial y} + \frac{1}{2} \mu \, c\lambda \, G(x) \, g(y) \frac{\partial F_0}{\partial y} = -\frac{1}{2} \mu \, c\lambda^2 \, T \, x \, G(x) \, h(y) \qquad (24)$$

$$\frac{\partial^2 F_1}{\partial x \, \partial y} + \frac{1}{2} \mu \, c\lambda \, G(x) \, g(y) \frac{\partial F_1}{\partial y} = \frac{\partial^2 F_0}{\partial x^2} - \frac{2F_0}{x^2} \qquad (25)$$

$$F_0 = \frac{\partial F_0}{\partial y} = F_1 = \frac{\partial F_1}{\partial y} = 0 \qquad \text{at } y = 0 \qquad (26)$$

These equations may be solved explicitly, since they are first-order linear equations in $\partial F/\partial y$. Introduce a function $a(y)$ by the relation

$$a(y) = \frac{1}{2} \mu c \lambda g(y) = 188 \lambda g(y) \tag{27}$$

The function $a(y)$ represents half the ratio between the characteristic length λ and the characteristic length $1/\mu$ $cg(y)$ associated with the magnitude of the conductivity. For large conductivities, $a(y)$ is a large number. For the data represented in Table 1, $a(y)$ has a maximum value 2×10^5 at y 5 (5 shakes), and exceeds 10^3 out to $y = 1000$ (10 microseconds).

The solution of Eq. (24) subject to the initial condition Eq. (26) is:

$$F_0(x,y) = -\frac{1}{2} \mu c \lambda^2 T \int_0^y dy' \, h(y') \int_0^x dx' \, x' \, G(x') \, e^{-a(y') \int_{x'}^{x} dx'' \, G(x'')}$$

$$\tag{28}$$

The lower limit of the x' integration has been set equal to zero to prevent the solution from becoming exponentially large at $x = 0$. The lowest-order field components are given by:

$$E_{\emptyset 0}(x,y) = -c \, B_{\theta 0}(x,y) =$$

$$-\frac{\mu c \lambda}{2 x} h(y) \int_0^x dx' \, x' \, G(x') \, e^{-a(y) \int_{x'}^{x} dx'' \, G(x'')}$$

$$\tag{29}$$

$$= -\frac{h(y)}{g(y)} \cdot \frac{a(y)}{x} \int_0^x dx' \, x' \, G(x') \, e^{-a(y) \int_{x'}^{x} dx'' \, G(x'')}$$

The factor $h(y)/g(y)$ is the Karzas-Latter solution. It is therefore necessary to study the properties of the remaining factor of Eq. (30), which will be called $W(x,y)$. First, since $a(y)$ and $G(x)$ are positive, $W(x,y)$ is positive. Therefore, the Karzas-Latter result that the magnetic field is augmented rather than excluded remains valid to this order of approximation. Second, an integration by parts brings W into the form:

$$W(x,y) = 1 - \frac{1}{x} \int_0^x dx' \; e^{-a(y) \int_{x'}^x dx'' \; G(x'')} \tag{30}$$

The integral appearing here is positive, so $W(x,y)$ is less than unity. Therefore, the Karzas-Latter solution is always greater than the solution obtained here.

A detailed study of the function $W(x,y)$ is presented in the Appendix. A simple approximate form, correct to about 1 per cent, has been obtained. Define a characteristic length $x_1(y)$ as:

$$a(y) = x_1(1 + x_1) \; e^{x_1} \tag{31}$$

For the data of Table 1, x_1 is between 4 and 8 over the range 1 shake to 10 microseconds. The length x_1 is the radius of the ionization sphere, which is thus between 1200 and 2400 meters. The function W is closely represented by

$$W(x,y) = 1 \qquad\qquad x \le x_1(y)$$
$$= \frac{x_1(y)}{x} \qquad\qquad x \ge x_1(y) \tag{32}$$

so the Karzas-Latter result is quite accurate.

The functions $x_1(y)$ and $h(y)/g(y)$ are plotted in Figs. 1 and 2 for the data of Table 1, and the time range $y < 7$. The current-conductivity ratio has been normalized by dividing by cB, producing a dimensionless number which can be regarded as a field susceptibility (perturbation magnetic field produced by electrons deflected by a unit magnetic field). For $y > 7$, the ratio $J_0/c\ B\ \sigma_0$ has the constant value 0.10.[*] This constancy is established by the exponential character of the decay, which may be expected for most nuclear explosions. This decrement constant is a very gradual function of the yield. The effective radius $x_1(y)$ decreases approximately linearly as y exceeds 7. The slope of the line is approximately .05 until values of x_1 less than unity are reached, which for the listed data, takes place at $y = 200$.

For the 1-MT explosion, the maximum value of $x_1(y)$ is 8. Therefore, for distances greater than $x = 8$ (2.4 km), the azimuthal electric and latitudinal magnetic fields rise to the maximum value $8\ J_0/\sigma_0\ x$, and then decrease linearly with time with slope .05. For x less than 8, the fields display a plateau, which begins when $x_1(y)$ first reaches x, and lasts until the second crossing.

The numerical constant which determines the asymptotic field strengths is given by:

---

[*]Karzas-Latter use 0.03 for this number. Discussions with R. Bjorklund and W. Karzas concerning the interpretation of the experimental data have established 0.10 as more accurate. Hence, the fact that our fields are 3.3 times Karzas-Latter's upper bound is a consequence of the choice of constants, and the analyses are consistent.
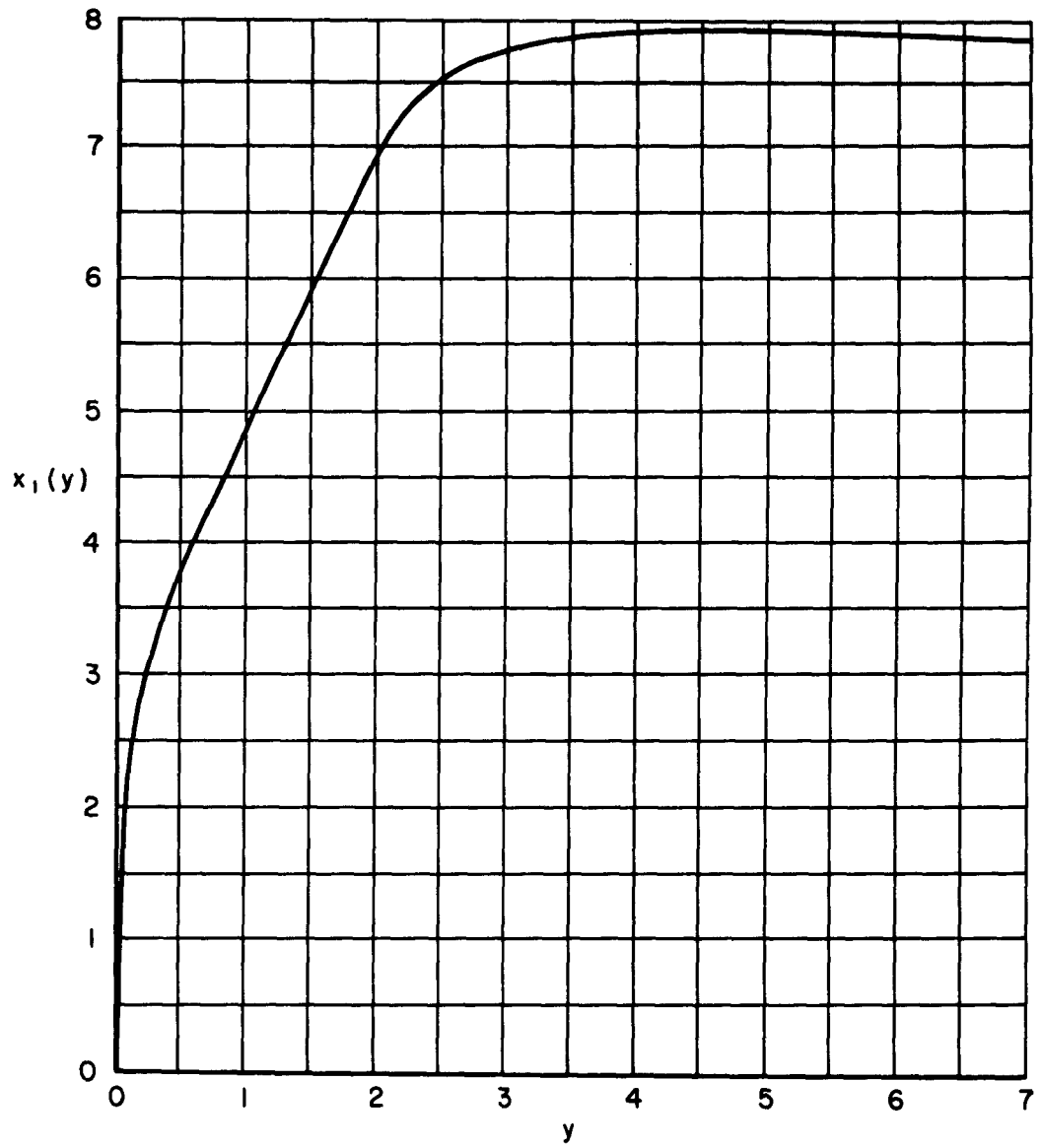
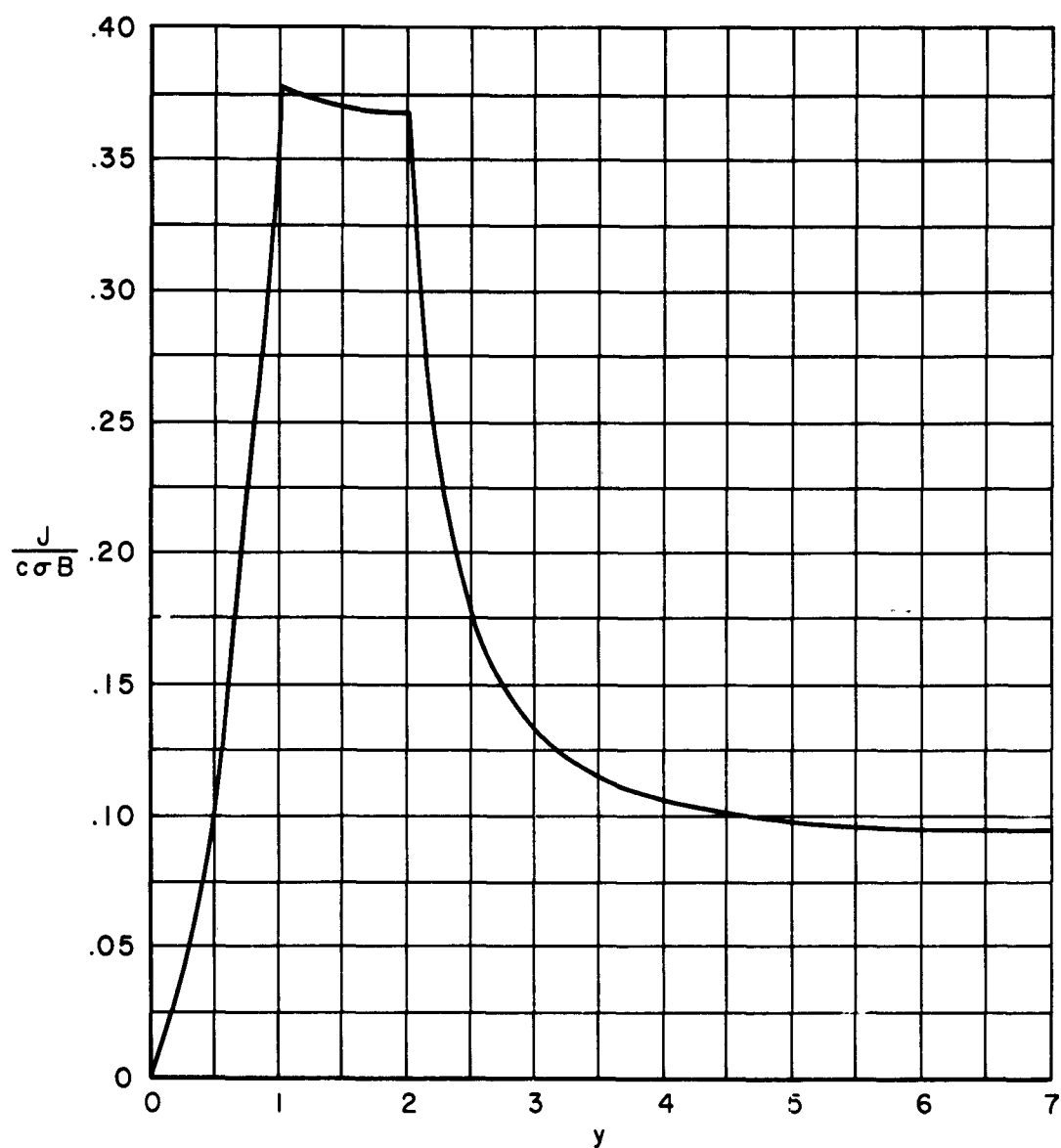Fig. I—Characteristic length $x_1(y)$ versus normalized retarded time

Fig. 2 — Current-conductivity ratio $\frac{J}{c\sigma B}$ versus normalized retarded time

$$\frac{J}{c \, \sigma \, B} \longrightarrow \frac{e}{m \, \omega_e} \cdot \frac{\gamma}{2} \cdot \frac{v_o}{c} \cdot \frac{R}{c} \cdot \frac{1}{q} = 0.10 \tag{33}$$

For Compton electrons, $\gamma = 2$, $v_o \sim c$. Here the gamma ray spectrum of the device has been employed. The mean range of the Compton is taken as 1 meter, corresponding to .44 MEV. This number is obtained from the mean energy resulting by integrating the Klein-Nishina scattering formula over the primary spectrum. The mobility is .20, and q is the ratio of the number of secondary to primary electrons (3×10^4). The insensitivity of the number to yield is apparent. (Dr. R. Bjorklund provided the required data for these numbers.) From the numbers presented here, it follows that the peak change in the vertical field is on the order of 10 per cent of the earth's magnetic field.

The field line structure will be perturbed by the current flow. The equation for the lines of the perturbation field is

$$\frac{dr}{rd\theta} = \frac{\Delta B_r}{\Delta B_\theta} = -\frac{2 \cos \theta}{\sin \theta} \frac{F}{r \, \partial F / \partial r} \tag{34}$$

which may be integrated to yield:

$$F(r,t) \sin^2 \theta = F(r_e, t) \tag{35}$$

where r_e denotes the value of r at which a particular field line crosses the equatorial plane $(\theta = \frac{\pi}{2})$.

The function F must be obtained by numerical integration. Equation (35) represents the field lines of a particular instant of time, where

F has been specified as a function of r and of $t - \frac{r}{c}$ by the wave

equation, Eq. (18), and its approximate solution Eq. (28). Accordingly,

the integration is quite complicated. The results are presented for

a time t = 10 microseconds after the initiation of the blast, at which

time the leading edge is at 3 km (10 x units). The function F should

not be taken too seriously for small values of x, although the general

behavior is correct. Figure 3 is a plot of F(x) at 10 microseconds.

Since F has a maximum, a field line must cut the equatorial

plane twice. Therefore, the lines close on themselves. The magni-

tude of the field strength varies along a given line, being largest

at the outer crossing. The perturbation field lines are plotted in

Fig. 4. These lines are arranged to have equal increments of field

strength at the outer crossing.

The lines are strongly crowded near the front, and spread as

we move inward. The line drawn closest to the front is actually that

on which the perturbation field strength at the outer crossing has

its largest value, 10 per cent of the earth's field. There are as

many lines between that line and the front as there are within that

line. Near the front, the field is predominantly in the latitudinal

direction, while at long distances within the front the field becomes

nearly radial, except at the equatorial plane. This general structure

holds for all times, though the details will vary as the front expands.

Next, we consider the higher approximations to the solution.

Equation (25) may be solved in exactly the same manner as Eq. (24),

and the same type of approximations made. The result is that the

field near the front is affected only very slightly by the second approxi-

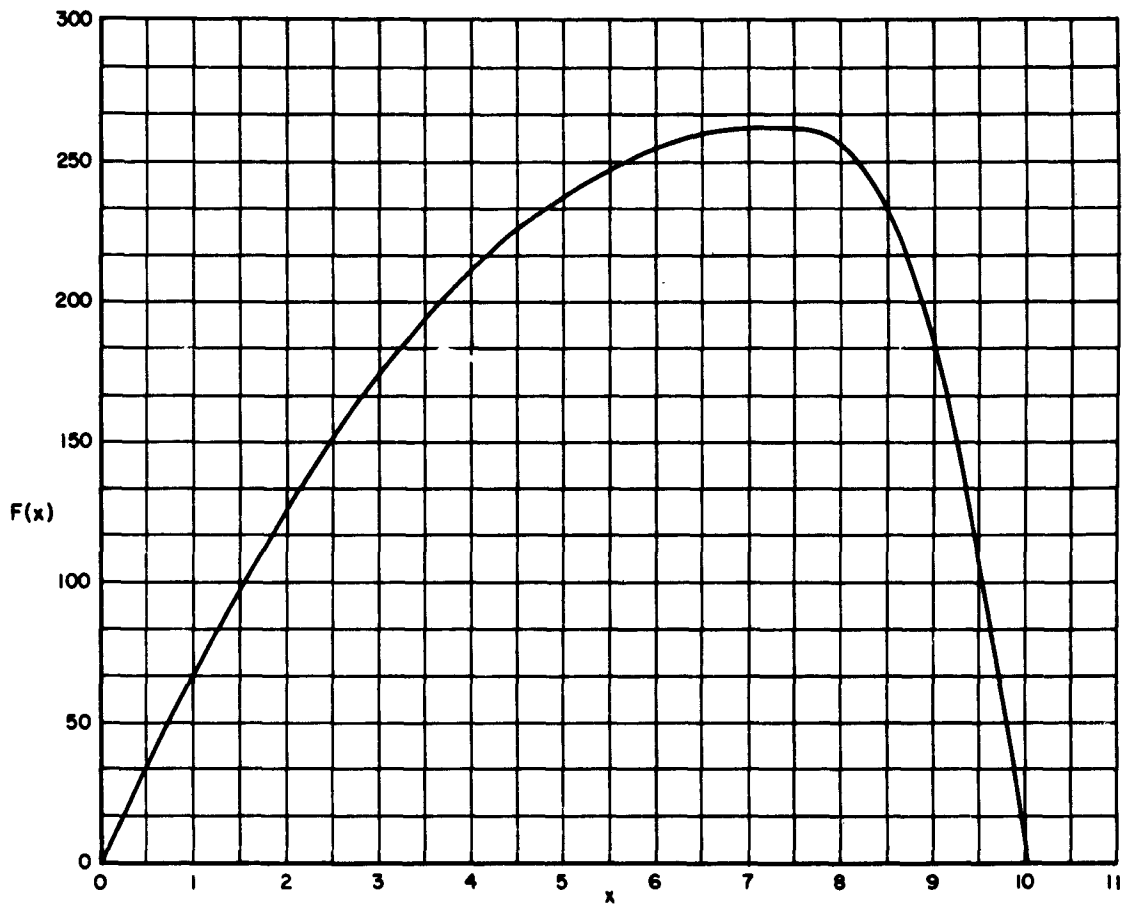mation. Farther back the effect is stronger, but the field is considerably
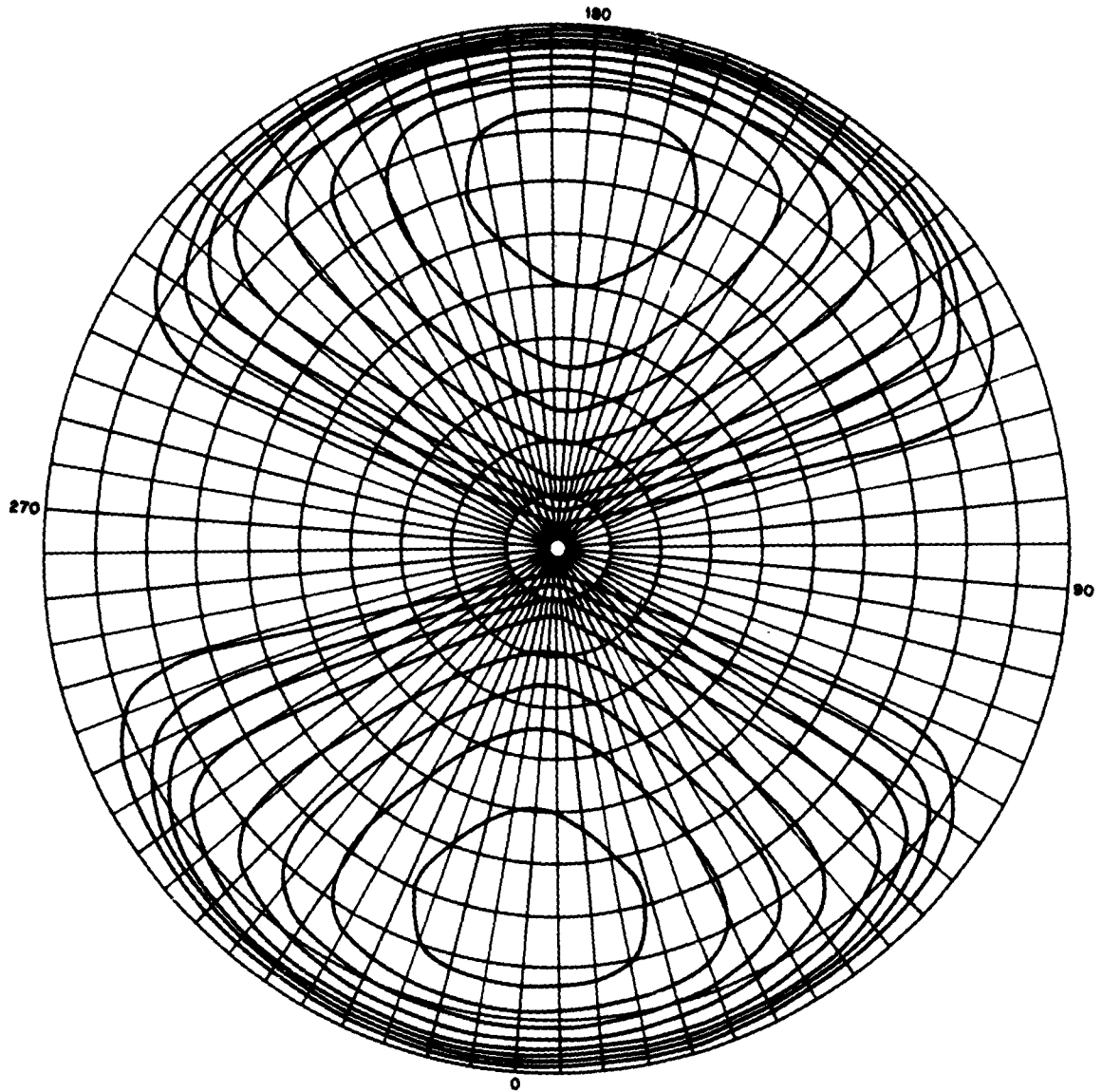
Fig. 3 — F (x) at t=10 μsec

Fig. 4 — The perturbation field lines at t=10 μsec

weaker. The higher approximations will contribute only about 1 per
cent of the total field, which is much less than the uncertainties in
the constants and in the validity of the general model. This result
means that the perturbation analysis is self-consistent. The peak
field is effectively independent of yield, but the "equivalent fire-
ball radius" x_1 depends logarithmically on yield.

In summary, the close-in electromagnetic fields produced by
deflection of Compton electrons in the earth's field have been analyzed,
and it has been shown that there is no significant exclusion or augmenta-
tion of the earth's field.

APPENDIX

The function $W(x,y)$ has been defined by Eqs. (3) and (29) as:

$$W(x,y) = \frac{a(y)}{x} \int_0^x dx' \, x' \, G(x') \, e^{-a(y) \int_{x'}^x dx'' \, G(x'')} \tag{36}$$

$$G(x) = e^{-x}/x^2 \tag{37}$$

The argument of a may be dropped, since W is a function of x and of a only. As x' approaches zero, the integral in the exponent tends to positive infinity, and the integrand tends to zero. The integral may be rewritten as:

$$W(x,y) = \frac{a}{x} \int_0^x dx' \, \exp - \left[x' + \log x' + a \int_{x'}^x G(x'') \, dx'' \right] \tag{38}$$

The expression in brackets is large for x' very large or very small. It therefore possesses a minimum, which may be called x_1. Call the bracketed expression $\psi(x')$. Differentiating and setting the result equal to zero yields:

$$\psi'(x_1) = 1 + \frac{1}{x_1} - a \, G(x_1) = 0 \tag{39}$$

$$a = x_1(1 + x_1) \, e^{x_1} \tag{40}$$

Equation (40) gives a as an explicit function of x_1, or x_1 as an implicit function of a. The solution of this implicit relationship has been plotted in Fig. 1 against y, using the relation between a and y defined in the text. The integral in the exponent may be written as:

$$\int_{x'}^{x} G(x'') \; dx'' = \int_{x'}^{\infty} G(x'') \; dx'' - \int_{x}^{\infty} G(x'') \; dx''$$

$$= I(x') - I(x) \tag{41}$$

Figure 5 gives I versus x and a versus x_1. For a positive, Eq. (40) has only one solution with x_1 positive.

The value of W will depend strongly on whether or not the minimum point x_1 is within the range of integration. If it is within, the integrand takes its largest value at $x = x_1$, and decreases rapidly as x moves away from x_1 in either direction. In this case, the integrand may be approximated by the well known method of steepest descent. The exponent is replaced by the first three terms of its Taylor series expansion about $x = x_1$, and the resulting expression yields a close approximation to the integral. There results:

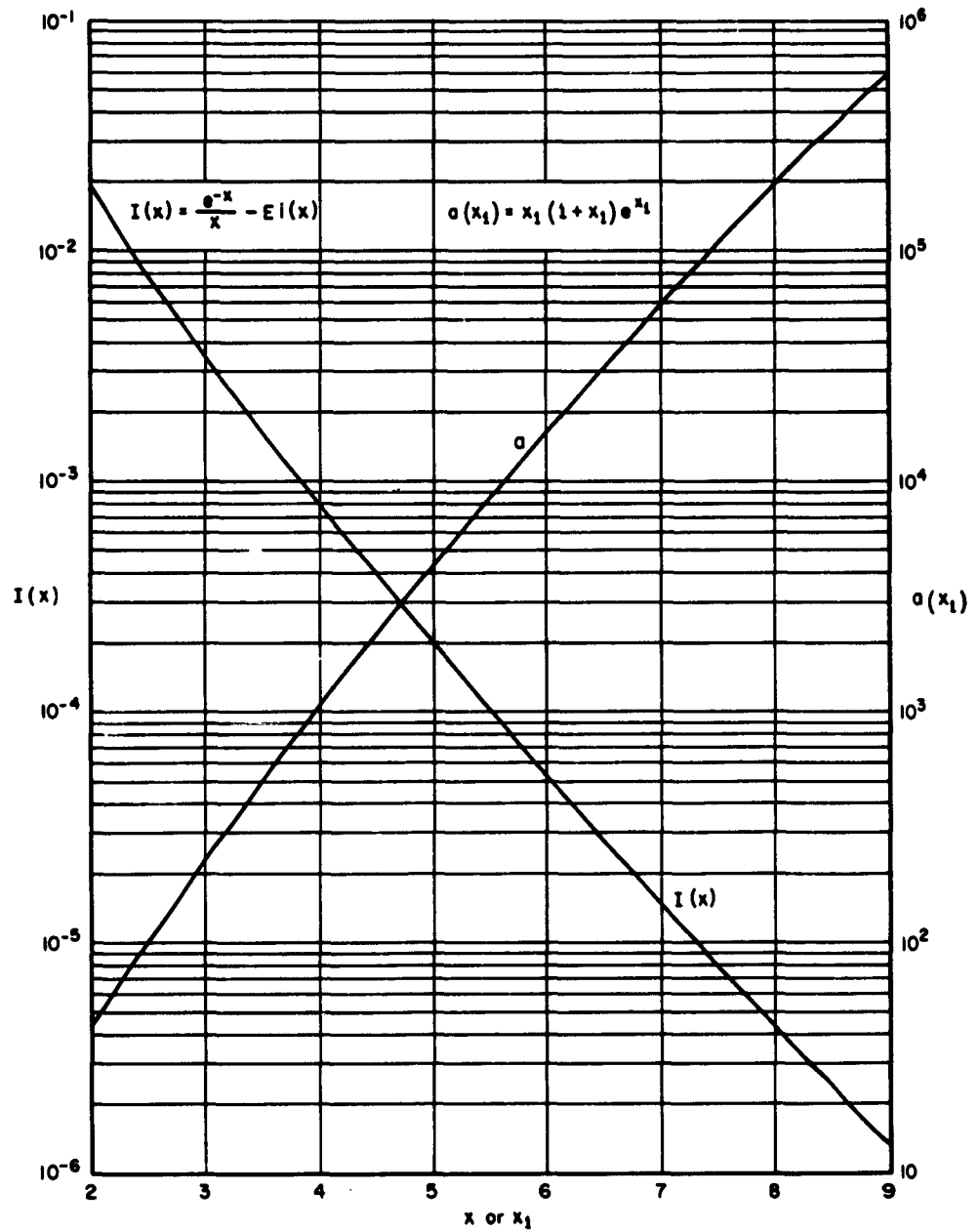$$W(x,y) \sim \frac{a}{x} \; e^{-\psi(x_1)} \int_{0}^{x} dx' \; e^{-\frac{1}{2} \psi''(x_1) (x' - x_1)^2}$$

Fig. 5 — The functions $I(x)$ and $a(x_1)$

Within the figure:

$I(x) = \dfrac{e^{-x}}{x} - EI(x)$

$a(x_1) = x_1(1+x_1)e^{x_1}$

$I(x)$

$a(x_1)$

x or x_1

$$W(x,y) \sim \frac{a}{x} e^{-\psi(x_1)} \sqrt{\frac{\pi}{2\psi''(x_1)}} \left[\text{erf}\left\{ \sqrt{\frac{\psi''(x_1)}{2}} (x - x_1) \right\} \right.$$

$$\left. + \text{erf}\sqrt{\frac{\psi''(x_1)}{2}} \ x_1 \right] \qquad (42)$$

where ψ'' denotes the second derivative of ψ, evaluated at x_1, and the error function erf is defined by:

$$\text{erf} \ z = \frac{2}{\sqrt{\pi}} \int_0^z du \ e^{-u^2} \qquad (43)$$

Equation (39) yields for the second derivative:

$$\psi''(x_1) = 1 + \frac{3}{x_1} + \frac{1}{x_1^2} \qquad (44)$$

For x_1 greater than 2, the argument of the second error function exceeds 2.34, and the function is between .999 and 1. The departure from unity may be neglected.

The first error function is zero at $x = x_1$, and increases rapidly to unity as x increases. Except for a small shoulder immediately above x_1, the sum of error functions may be set equal to 2. The remaining factors have been studied numerically. The variation of ψ with x_1 arising from th. term $I(x)$ tends to cancel the variation of the error function terms near $x = x_1$. For x significantly larger than x_1, $I(x)$ becomes negligible. The other parts of W depend on x_1 only. The details yield:

$$W(x,y) \sim \frac{x_1(y)}{x} \qquad\qquad x > x_1(y) \qquad\qquad (45)$$

For x less than x_1, the minimum is not within the range of integration. The largest values of the integrand now occur at the end point $x' = x$. Again expanding the exponent, but now around the end point, there results:

$$W(x,y) \sim \frac{a}{x} e^{-\psi(x)} \int_0^x dx' \, e^{-\left[\psi'(x)(x'-x) + \frac{1}{2}\psi''(x)(x'-x)^2\right]} \qquad (46)$$

$$\sim a \, G(x) e^{\frac{1}{2}\frac{[\psi'(x)]^2}{\psi''(x)}} \frac{\sqrt{\pi}}{\sqrt{2\psi''(x)}} \left[\text{erf}\left\{ \sqrt{\frac{\psi''(x)}{2}} \left(x + \frac{|\psi'(x)|}{\psi''(x)} \right) \right\} \right.$$

$$\left. - \, \text{erf}\, \frac{|\psi'(x)|}{\sqrt{2\psi''(x)}} \right] \qquad (47)$$

Here, the arguments of both error functions are large. The difference, multiplied by the exponential, yields an algebraic function. A numerical study shows that the resulting expression varies by only a few per cent for x ranging from 0 to 7, which is the largest value of x_1 in the detailed problem. Thus, the expression may be set equal to unity, since it must be continuous. Therefore, the function W is given by:

$$W(x,y) = 1 \qquad\qquad x < x_1(y)$$

$$= \frac{x_1(y)}{x} \qquad\qquad x > x_1(y) \tag{48}$$

This expression is in error by only a few per cent over the complete range.

REFERENCES

1. Mark, J.C., "The Detection of Nuclear Explosions," Nucleonics, Vol. 17, August 1959, p. 64.

2. Kompaneets, A.S., "Radio Emission from an Atomic Explosion," J. Exptl. Theoret. Phys. (Soviet Physics JETP), Vol. 35, No. 6, June 1959, p. 1076.

3. Liepunskii, O.I., "Possible Magnetic Effects from High-Altitude Explosions of Atomic Bombs," J. Exptl. Theoret. Phys. (Soviet Physics JETP), Vol. 38, 1960, p. 302.

4. Johnson, M.H. and B.A. Lippmann, "Electromagnetic Signals from Nuclear Explosions in Outer Space," Phys. Rev., Vol. 119, No. 3, August 1, 1960, p. 827.

5. Karzas, W.J., and R. Latter, "Electromagnetic Radiation from a Nuclear Explosion in Space," Phys. Rev., Vol. 126, No. 6, June 15, 1962, p. 1919.

6. Karzas, W.J., and R. Latter, "The Electromagnetic Signal due to the Interaction of Nuclear Explosions with the Earth's Magnetic Field," Journ. Geophys. Res., Vol. 67, No. 12, November 1962, p. 4635.

7. Nielsen, R.A. and N.E. Bradbury, "Electron and Negative-Ion Mobilities in Oxygen, Air, Nitrous Oxide, and Ammonia," Phys. Rev., Vol. 51, 1937, p. 69.

8. Crompton, R.W. and D.J. Sutton, "Experimental Investigation of the Diffusion of Slow Electrons in Nitrogen and Hydrogen," Proc. Roy. Soc., Series A, Vol. 215, 1952, p. 467.

9. Crompton, R.W. and L.G.H. Huxley and D.J. Sutton, "Experimental Studies of the Motions of Slow Electrons in Air with Application to the Ionosphere, Proc. Roy. Soc., Series A, Vol. 218, 1953, p. 507.

10. Chanin, L.M., A.V. Phelps and M.A. Biondi, "Measurements of the Attachment of Low-Energy Electrons to Oxygen Molecules," Phys. Rev., Vol. 128, No. 1, October 1, 1962, p. 219.